

Waste Water Ammonia Stripping Intensification Using Microfluidic System

M. H. Almasvandi, M. Rahimi*

CFD Research Center, Chemical Engineering Department, Razi University, Kermanshah, Iran

ARTICLE INFO

Article history:

Received: 2016-07-18

Accepted: 2016-11-10

Keywords:

Air Stripping

Ammonia

Microchannel

Optimization

Overall Volumetric Mass

Transfer

ABSTRACT

This paper reports the results of experimental removal process of ammonia from synthetically prepared ammonia solution using a microscale mixing loop air stripper. Effects of various operational parameters (such as pH, air flow rate, wastewater flow rate, and initial ammonia concentration) were evaluated. By increasing pH from 10 to 12.25, the amount of K_{La} increased from 0.26 to 0.73 h^{-1} . Considerable enhancement, about 150 %, can be found for K_{La} by changing the air flow rate from 280 to 700 mL/min under a fixed condition. The wastewater flow rate can also increase the value of K_{La} from 0.22 to 0.59 h^{-1} . The values of K_{La} increased only about 20 % by changing the initial concentration of ammonia in the range between 50 and 500 mg/L. The results showed that any improvement concerning air stripping using microchannel was successfully carried out with enhancing the overall volumetric mass transfer coefficient (K_{La}) and providing higher mass transfer capabilities compared with other types of strippers, even for lower amounts of used air. The enhancement of mass transfer takes place by efficient mixing induced by the employed microchannel. It has been demonstrated that wastewater flow rate and air flow rate have significant effects on K_{La} . The optimal stripping conditions and mathematical modeling for ammonia removal and the relation between the parameters were determined using Response Surface Methodology (RSM) with Central Composite Design (CCD) method. The results demonstrate the advantages the proposed system possesses over conventional stripper types.

1. Introduction

Major environmental problems in industrial wastewaters are the result of ammonia and its compounds. Even small amount of ammonia has negative effects on aquatic life when it is discharged without any treatment. The recovery and removal of ammonia and its components from wastewaters can be

accomplished by biological, physical, and chemical processes and combination of these methods such as adsorption, chemical precipitation, membrane filtration, reverse osmosis, ion exchange, air stripping, breakpoint chlorination, and biological nitrification. The treatment of the ammonia from wastewaters by biological processes is

*Corresponding author: m.rahimi@razi.ac.ir

normally complex [1].

Air stripping is effectively applied to the removal of nitrogen from different wastewaters such as pig slurry [2], landfill leachate [3], and wastewaters from the production of mineral fertilizers [4]. Air stripping has many applications in physical-chemical process so as to remove ammonia from wastewaters. The transfer is accomplished by the interaction of the high concentration liquid ammonia with air, which has no ammonia initially [5, 6].

There are various air stripping systems such as bubble aeration [3], packed tower [7, 8], water-sparged aerocyclone (WSA) [9], micro-fabricated stripping column [10], and jet loop reactor (JLR)[1]. Ammonia is soluble in water and its volatility decreases with decreasing temperature. Hence, effective air stripping requires intermediate temperatures and uses large volumes of air. Several types of gas-liquid microchannel have been investigated for a number of chemical reactions [11-14]. They can be classified according to their phase contacting principle into continuous and dispersed contacting [15]. The use of microchannel gas-liquid contactor is an alternative to further improve the gas-liquid mass transfer for the stripping process [16, 17]. Low inventories in microchannels make them attractive to carry out reactions which have an explosion tendency and involve hazardous and toxic chemicals. Thus, in case of an accident, the potential harm to the operator and environment would be limited [18, 19]. Microchannels are characterized by high surface-to-volume ratio. Microchannels can be very useful for two-phase reactions, gas-liquid and liquid-liquid mass transfer operations, as transfer paths are minimal and specific interfacial areas are very high [20-24]. Several studies in the field of

gas-liquid mass transfer [25-29] and liquid-liquid mass transfer [30-32] in microchannels have also been reported.

The microchannels have more advantages in comparison with classical reactors. These advantages are mainly the lower required time for process, simple construction, and lower operational costs, causing lower operational costs. Microchannel reactor as a continuous reactor is interesting due to high volume/surface ratio, higher transport rates (i.e., heat and mass transfer rates), short diffusion distance, and simple required process control [33-35]. Due to the higher internal mixing and larger contact area in microchannels, mass transfer coefficients are higher than classical type reactors [36-39]. Considering the above-mentioned specifications of microchannels, volatile chemicals may be transferred rapidly to the gas phase from the liquid phase.

Determination of the optimum condition in a process by Response Surface Methodology (RSM) is widely reported in literature [23, 28, 40-42]. Bashir et al. [28] reported the application of RSM for optimization of ammoniacal nitrogen removal of semi-aerobic landfill leachate using ion exchange resin. They used RSM to evaluate the effects of process variables and interactions towards the attainment of optimum conditions. Hossini et al. [30] optimized ammonia volatilization using air stripping from aquatic solutions using response surface methodology.

In the present study, a microchannel with T-shaped junction was used as a stripper for ammonia removal of wastewater by air stripping. The experiments were carried out to investigate the influences of process variables including pH, air flow rate (Q_{air}), wastewater flow rate (Q_{water}), and initial ammonia concentration (C_0) on $K_{L,a}$. The advantage of

using microfluidic system was evaluated by comparing the overall mass transfer coefficient with the other type of strippers. The operational condition was then optimized using RSM. The relevant resulted optimal conditions for removal of ammonia and the relation between the parameters were determined using central composite design (CCD) method.

2. Materials and method

2.1. Materials and chemicals

In this study, all the employed chemicals were supplied for Merck Company (Germany), and the solutions were prepared with freshly double distilled water. An aqueous 25 % solution of ammonia was used to prepare the synthetic wastewaters with different concentrations of ammonia 50-500 mg/L. Sodium hydroxide (NaOH) and sulfuric acid (H₂SO₄) were used to adjust pH.

The concentration of ammoniacal nitrogen (NH₃-N) was measured by Nessler Method using a UNICO UV-2100 spectrophotometer. The wavelength of the spectrophotometer was set at 420 nm.

2.2. Experimental setup

The air stripping of ammonia from wastewater was carried out by a microfluidic system, which is shown in Fig. 1. Compressed air was supplied by an air compressor and was entered into one side of the T-shaped junction. A valve was erected to control the volumetric flow rate of air, and it was monitored by an air flow meter. The gas flow rate was controlled within 280-700 mL/min. The synthetic wastewater containing ammonia, after passing through a water bath, was then pumped into the other side of T-shaped junction by a dosing peristaltic pump (QIS DSP 100). The mixture of air and wastewater was driven into the microchannel, with 50 cm length and 600 μm internal diameter, to allow desorption of ammonia from wastewater to air due to strong mixing inside the channel. A tube was erected at the top of the separator to exhaust the waste gas. The separator was employed to trap and recycle the droplets of the liquid carried by the waste gas.

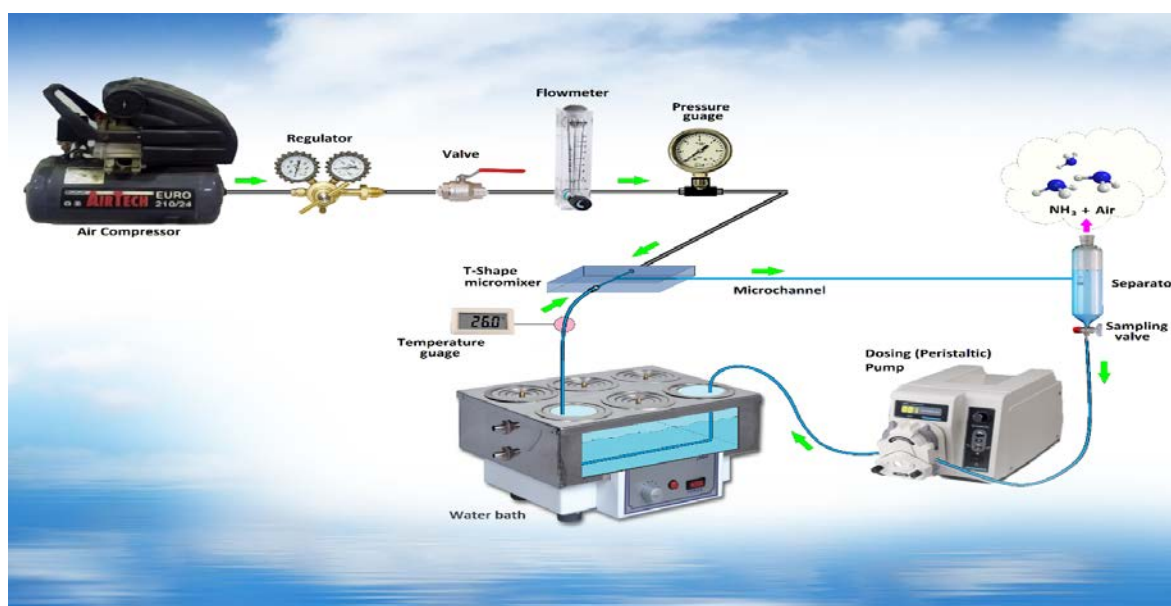


Figure 1. The flow diagram of the experimental setup.

2.3. Experimental procedure

In all stages of the experiments, 100 mL of the synthetic wastewater with different concentrations of ammonia was prepared just before experiments, and NaOH was added to adjust the pH of liquid phase. Temperature of air and synthetic wastewater were kept constant during the experiments at 25 °C.

The experiments were carried out in the batch mode. Prior to each run, the water tank (separator) was filled with 100 mL of synthetic wastewater. Then, the compressed air was allowed to enter the T-shaped junction at a prescribed flow rate. When the gas phase pressure reached a steady-state condition, the circulation dosing pump at a certain flow rate pumped the liquid phase from the separator into the T-shaped junction. During the circulation, total concentration of ammonia in the water was measured at outlet of the separator, while the concentration continuously decreased.

In order to understand the overall performance of the process, the effect of some experimental variables was investigated on the mass transfer coefficient of ammonia. These variables are the flow rates of air and wastewater, initial concentration of ammonia, and pH of the solution.

2.4. Physical mass transfer coefficient calculation

The mass transfer rate of volatile compound, A, from liquid phase into a batch gas stripping unit can be evaluated by Matter and Muller equation [43]:

$$-Ln\left(\frac{C_{At}}{C_{A_0}}\right) = \left(\frac{Q_G H_A}{V_L}\right) \left(1 - \text{Exp}\left(-\frac{K_L a V_L}{Q_G H_A}\right)\right) t \quad (1)$$

where C_{At} and C_{A_0} are the liquid phase

concentrations of compound A (g/m^3), at any time (t) and at the beginning of experiment, respectively. In addition, H_A is the dimensionless Henry's constant; K_L is the overall liquid mass transfer coefficient (m/min); a is the interface area per unit volume of liquid (m^2/m^3); V_L is the total volume of liquid (L); Q_G is the gas flow rate (L/min), and t is the stripping time (min).

When the exiting stripping gas is far from saturation, $K_L a V_L / H_A Q_G \ll 1$; hence, Eq. (1) will be simpler:

$$-Ln\left(\frac{C_{At}}{C_{A_0}}\right) = K_L a t \quad (2)$$

Since ammonia is an easily soluble gas, the exiting stripping gas may possibly be far from saturation condition because of the very short residence time of the stripping in the microchannel. Therefore, the mass transfer coefficient of ammonia removal was tentatively obtained according to Eq. (2) [9].

3. Results and discussion

The T-shape micromixer mixes both of the air and the liquid leading to forming a good mixture of two phases inside the microchannel. Mass transfer between gas and liquid takes place in the interfacial area. The efficient mass transfer in microchannel may be the result of high volume/surface ratio and short diffusion distance between gas and liquid.

3.1. Effect of operational conditions on $K_L a$

In this study, the effects of some operational variables, such as pH, Q_{air} , Q_{water} , and C_0 , are investigated on the amount of $K_L a$. The effect of each parameter is evaluated while the other parameters are at constant values.

3.1.1. Effect of pH

The pH may affect the ammonia volatilization. NH_3 (g) and NH_4^+ (aq) are in equilibrium at about pH 9. The higher pH may force more NH_4^+ into the gas phase.

Thus, ammonia is rarely noticed at the acidic pH, and adding NaOH to their solutions will increase the ammonia volatilization. The equilibrium relationship is shown in Fig. 2 [44, 45].

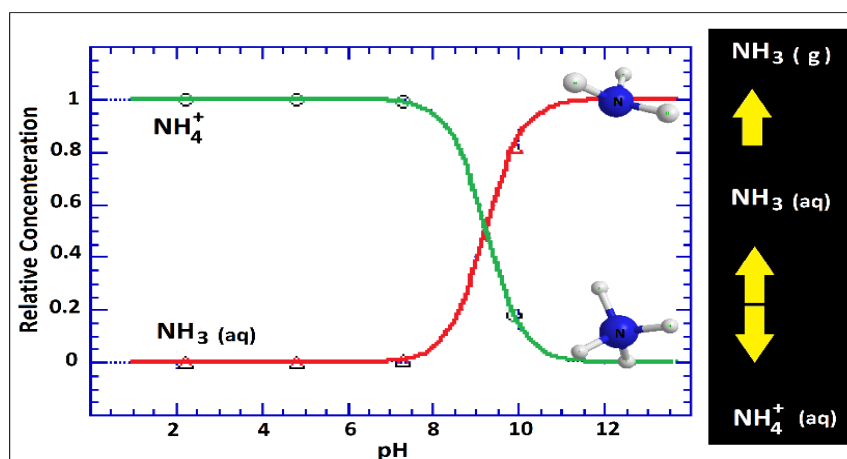


Figure 2. Effect of pH on the equilibrium relationship between NH_3 (aq) and NH_4^+ .

Various solutions of the synthetically prepared ammonia with different pHs were used to evaluate the effect of pH on $K_{L}a$. The employed pHs were 10, 10.75, 11.5, 12.25, and 13. In this step, air and wastewater were used at constant flow rates, 595 and 5.68 mL/min, respectively; further, the initial ammonia concentration was 387.5 mg/L. Fig. 3 shows that by increasing the pH value from 10 to 12.25, the amount of $K_{L}a$ will increase; it can be easily separated from wastewater due to generating more ammonia. Increasing the pH beyond 12.25 does not have any important effect on $K_{L}a$.

3.1.2. Effect of air flow rate

The effect of air flow rate on $K_{L}a$ is illustrated in Fig. 4. The results show that $K_{L}a$ increases with increasing Q_{air} in the employed range. As this figure reveals, the values of $K_{L}a$ vary between 0.24 and 0.61 h^{-1} by changing the air flow rate from 280 to 700 mL/min; under fixed values of pH 11.5, wastewater flow rate was 5.68 mL/min and initial ammonia

concentration was 387.5 mg/L. This effect can be explained by high dissolution of ammonia in water phase; hence, the overall mass transfer resistance to the ammonia removal process is mainly on the gas film side; therefore, the overall mass transfer resistance can be reduced by increasing the gas flow rate. Mass transfer reduction brings about increased gas entrainment and gas-liquid interfacial area, thus increasing $K_{L}a$ [39].

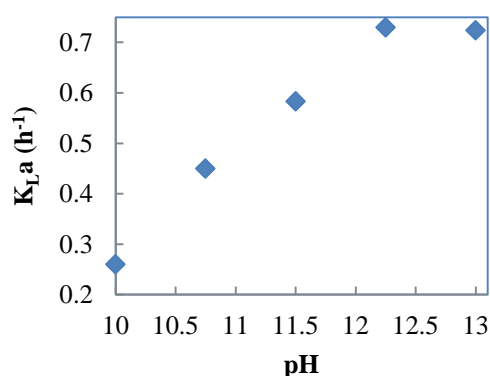


Figure 3. Effect of pH on $K_{L}a$.

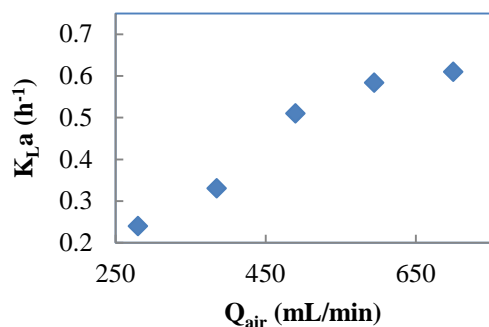


Figure 4. Effect of air flow rate on $K_{L,a}$.

3.1.3. Effect of wastewater flow rate

As depicted in Fig. 5, the increased wastewater flow rate from 0.25 to 7.5 mL/min leads to an increase in $K_{L,a}$ at fixed values of pH 11.5, air flow rate of 595 mL/min, and initial ammonia concentration of 387.5 mg/L. Any changes in the wastewater flow rate may lead to the development of the gas-liquid interfacial area and, hence, enhancement of the mass transfer. The increasing wastewater flow rate results in a higher removal rate due to higher concentration gradient and mass transfer rate. The amount of $K_{L,a}$ will increase until reaching a specific flow rate of wastewater, i.e., 5.68 mL/min herein. A constant amount will be found beyond this flow rate.

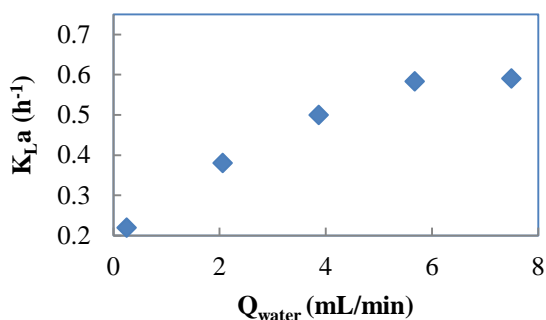


Figure 5. Effect of wastewater flow rate on $K_{L,a}$.

3.1.4. Effect of initial concentration of ammonia

The influence of initial concentration of ammonia, C_0 , on $K_{L,a}$ is shown in Fig. 6. The

figure depicts a slight increase in $K_{L,a}$ with increasing initial concentration of ammonia in the range of 50 to 500 mg/L, under the fixed values of pH 11.5, as well as air and wastewater flow rates equal to 595 and 5.68 mL/min, respectively. This behavior may be due to the driving force required for the mass transfer, which is increased with increasing C_0 . This effect shows that the removal of ammonia is mainly controlled by the ammonia diffusion into the gas film as explained in the literature [1].

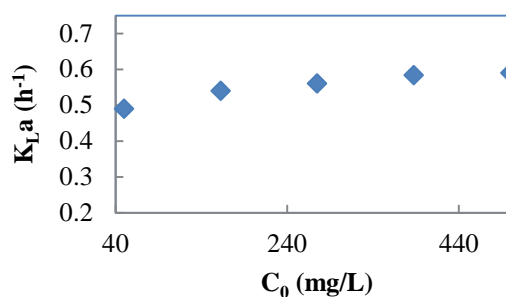


Figure 6. Effect of initial ammonia concentration on $K_{L,a}$.

3.2. Comparison with the other types of strippers

The air consumption per unit volume of wastewater and $K_{L,a}$ are compared with respect to microchannel, JLR, stirrer tank, packed tower, and WSA in Table 1. The calculated values of $K_{L,a}$ in microchannel are higher than those of stirred tank reactors, JLR and packed towers. However, they are lower than those of WSA. It should be considered that air consumptions of tank reactor, packed tower, and WSA reactor are 1.1–16 fold of microchannel. Good mixing and increasing interfacial surface are the main reasons for the priority of microchannel compared with other types of the strippers. These improvements also cause a significant increase in mass transfer rate between the two phases and provide higher $K_{L,a}$ with less air consumption.

Table 1

The comparison of air consumption and K_La in different equipment.

Equipment	Experimental conditins			Air consumption air(L/min)/liquid(L)	K_La (h^{-1})	Reference
	V_L (L)	Q_G (L/min)	T (°C)			
Microchannel	0.100	0.595	20	5.95	0.73	This work
JLR	9	50	20	5.5	0.63	[1]
Stirrer tank	0.05	4.8	16	96.0	0.48	[8]
Packed tower	1000	25000	15	25.0	0.42	[1]
WSA	10	66	15	6.6	0.78	[9]

This comparison shows that the microchannel consumed less air than tank reactor, packed tower and WSA reactor with respect to per unit volume of treated wastewater. Moreover, scaling and fouling on the packing surface in packed towers and lower stripping efficiency are the most prominent problems in packed tower.

3.3. Experimental design, analysis and optimization

The optimization and mathematical modeling of this work was performed using Design Expert Software [46]. The Central Composite Design (CCD) was used to model the process. The independent factors used in this study are pH, Q_{air} , Q_{water} , and C_0 coded as A, B, C, and D, respectively (Table 2). The independent factors varied over five levels ($-\alpha$, -1 , 0 , 1 , $+\alpha$), and their ranges were determined based on preliminary studies and literature review.

Table 2

Experimental ranges and levels of independent process variables.

Independent variable	Code	$-\alpha$	-1	0	$+1$	$+\alpha$
pH	A	10	10.75	11.5	12.25	13
Q_{air} (mL/min)	B	280	385	490	595	700
Q_{water} (mL/min)	C	0.25	2.06	3.87	5.68	7.5
C_0 (mg/L)	D	50	162.5	275	387.5	500

As there are only five levels for each factor, the appropriate model is quadratic model Eq. (3).

$$Y = \beta_0 + \sum_{j=1}^k \beta_j X_j + \sum_{j=1}^k \beta_{jj} X_j^2 + \sum_i \sum_{j \geq i} \beta_{ij} X_i X_j + e_i \quad (3)$$

where Y is the response, X_i and X_j are the variables, β_0 is a constant coefficient, β_j , β_{jj} , and β_{ij} are the interaction coefficients of linear, quadratic, and second-order terms, respectively, k is the number of studied factors, and e_i is the error.

The coefficient of determination (R^2) was used to identify the quality of the fit of polynomial model, and the P-value associated with the 95 % confidence level was used to evaluate the variables and the interactions between them. The significance and adequacy of the model was assessed according to the calculated F-value (Fisher variation ratio), probability value (Prob>F), and adequate Precision. Finally, the values of response variables (pH, Q_{air} , Q_{water} , and C_0) were compared in an overlay plot to identify the optimum region of mass transfer coefficient.

In the current study, 30 CCD batch runs were conducted totally. The operational conditions, experimental and predicted K_{La} are listed in Table 3. Using these experiments, the values of K_{La} were found in the range of 0.083 through 0.730 h^{-1} . As illustrated in this table, K_{La} reached its maximum value of 0.730 h^{-1}

under stripping condition of Q_{water} as 5.68 mL/min, Q_{air} as 595 mL/min, C_0 as 387.5 mg/L, and pH as 12.25. However, the higher rates of air flow will increase the amount of K_{La} . This observation is in agreement with previous reports [47].

Table 3

Results of the central composite design.

Run	Process variable				Responses $K_{La} (\text{h}^{-1})$	
	A: PH	B: Q_{air} (mL/min)	C: Q_{water} (mL/min)	D: C_0 (mg/L)	Actual	Predicted
1	11.5	490	3.87	50	0.390	0.353
2	12.25	385	2.06	387.5	0.220	0.229
3	11.5	490	0.25	275	0.099	0.098
4	12.25	385	5.68	387.5	0.421	0.417
5	11.5	490	3.87	275	0.360	0.396
6	11.5	490	3.87	275	0.399	0.396
7	10.75	595	5.68	162.5	0.544	0.518
8	12.25	595	2.06	162.5	0.320	0.349
9	10.75	385	5.68	387.5	0.310	0.326
10	11.5	280	3.87	275	0.235	0.197
11	12.25	385	5.68	162.5	0.234	0.267
12	11.5	490	3.87	275	0.440	0.396
13	10.75	595	2.06	387.5	0.285	0.264
14	11.5	490	3.87	275	0.380	0.396
15	10.75	595	2.06	162.5	0.310	0.329
16	12.25	595	5.68	162.5	0.532	0.537
17	12.25	595	2.06	387.5	0.487	0.499
18	12.25	385	2.06	162.5	0.083	0.078
19	10.75	385	2.06	162.5	0.178	0.203
20	10.75	385	5.68	162.5	0.356	0.391
21	11.5	490	3.87	500	0.387	0.438
22	12.25	595	5.68	387.5	0.730	0.687
23	11.5	490	3.87	275	0.398	0.396
24	11.5	490	7.5	275	0.487	0.475
25	13	490	3.87	275	0.410	0.399
26	10.75	385	2.06	387.5	0.190	0.138
27	11.5	700	3.87	275	0.602	0.594
28	10	490	3.87	275	0.290	0.288
29	10.75	595	5.68	387.5	0.432	0.453
30	11.5	490	3.87	275	0.393	0.396

3.3.1. Regression model equation and analysis of variance (ANOVA)

Table 4 shows the analysis of variance (ANOVA) of regression parameters of the predicted response surface quadratic model for K_{La} . As is clear in Table 4, the F-value of model is 74.66, and a low probability value ($P < 0.0001$) indicates the significance of the model. Values of $P > F$ less than 0.05 indicate that model terms are significant, while values greater than 0.1 indicate that the model terms are not significant [48]. The “Adequate Precision” ratio of the model was found 35.995 (Adequate Precision > 4), which is an adequate signal for the model [49]. The lack of fit F-statistic was statistically significant as the P-values were less than 0.05. A significant lack of fit suggests that there may be some systematic variations unaccounted for in the hypothesized model. This may be due to the exact replicate values of the independent variable in the model that

provide an estimate of pure error. The value of correlation coefficient ($R^2=0.966$) obtained in the present study for K_{La} was higher than 0.80, indicating that only one point of the total dissimilarity might not be explained by the empirical correlation (according to Joglekar [50], for a good fit of a model, the correlation coefficient should be at a minimum of 0.80). High value of R^2 illustrates good agreement between the calculated and observed results within the range of experiment. In this study, A, B, C, D, AB, AD, A^2 , and C^2 are significant model terms. Insignificant model terms, which have limited influence, such as B^2 , D^2 , AC, BC, BD, and CD, were excluded because their P-values are equal to 0.5110, 0.5898, 0.3344, 0.1679, 0.6360, and 0.6253, respectively. Based on the results, the RSM constructed in this study for predicting K_{La} was considered reasonable.

Table 4
ANOVA used for analysis of variance and adequacy of the quadratic model.

Source	Sum of squares	Degree of freedom	Mean square	F-Value	(P-Value)
Model	0.569787	8	0.071223	74.66253	< 0.0001
A-pH	0.01826	1	0.01826	19.14191	0.0003
B- Q_{air}	0.236414	1	0.236414	247.8294	< 0.0001
C- Q_{water}	0.213194	1	0.213194	223.4881	< 0.0001
D- C_0	0.010923	1	0.010923	11.4501	0.0028
AB	0.020592	1	0.020592	21.5866	0.0001
AD	0.046225	1	0.046225	48.4571	< 0.0001
A^2	0.004877	1	0.004877	5.112179	0.0345
C^2	0.021267	1	0.021267	22.29432	0.0001
Residual	0.020033	21	0.000954		
Lack of Fit	0.016529	16	0.001033	1.474089	0.3539
Pure Error	0.003504	5	0.000701		

SD=0.0308, PRESS=0.0392, $R^2=0.966$
 $R^2_{adj}=0.953$, Adeq Precision=35.995.

In terms of actual variables, an empirical relationship between K_{La} and process

variables can be expressed by the following equation.

$$K_{La} = 0.63417 + 0.17376 \times PH - 0.00429365 \times Q_{Air} + 0.11667 \times Q_{Water} - 0.00713630 \times C_0 + 0.000455556 \times PH \times Q_{Air} + 0.000637037 \times PH \times C_0 - 0.023278 \times PH^2 - 0.00834643 \times Q_{Water}^2 \quad (4)$$

As shown in Fig. 7, the predicted values of K_{La} obtained from the model and the actual experimental data are in good agreement [51].

The 3D surface response and contour plots of the quadratic model were utilized to assess the interactive relationships between independent variables and K_{La} . As Figs. 8 and 9 show, two variables were kept constant, while the other two varied within the experimental ranges.

As it is depicted in Figs. 8 and 9, the influences of Q_{air} and Q_{water} on K_{La} were more significant than those of pH and C_0 , which showed limited effects.

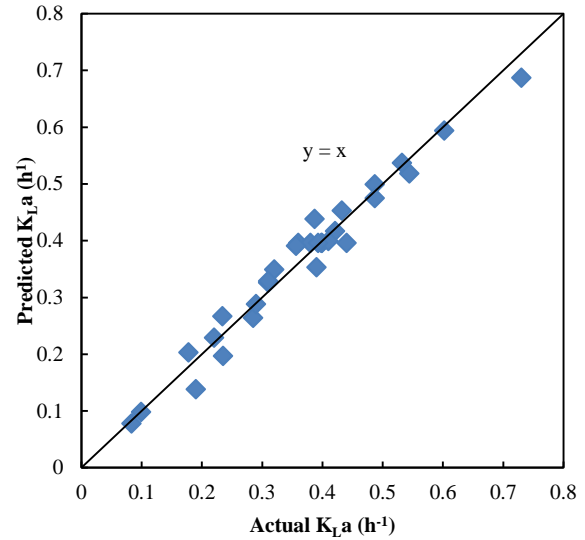


Figure 7. Predicted versus actual values for K_{La} .

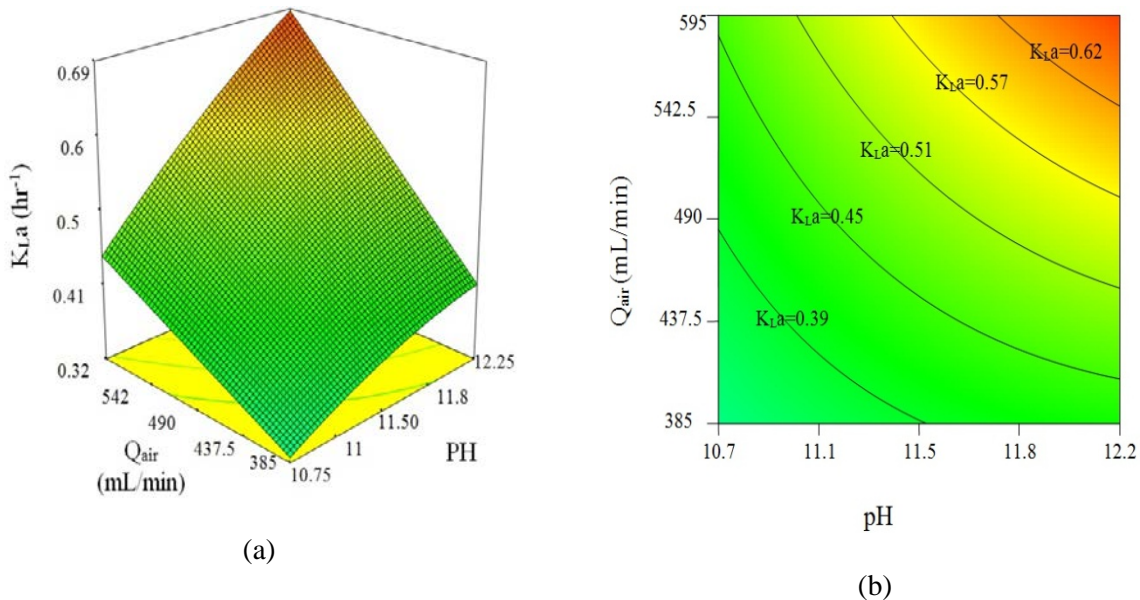


Figure 8. (a) Response surface and (b) contour plots for K_{La} as a function of pH and Q_{air} (Q_{water} of 5.68 mL/min and C_0 of 387.5 mg/L).

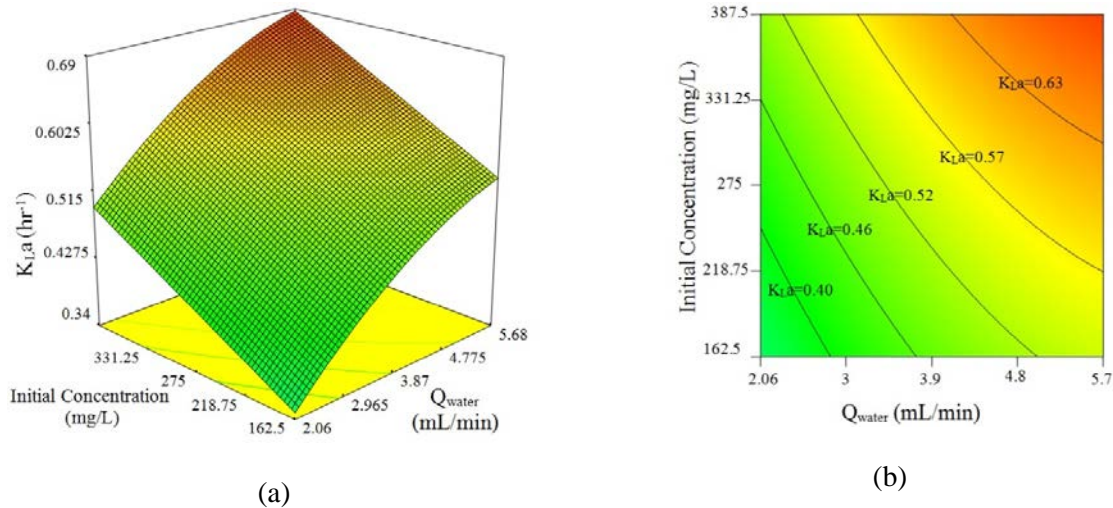


Figure 9. (a) Response surface and (b) contour plots for K_{La} as a function of Q_{water} and C_0 (Q_{air} of 595 mL/min and pH of 12.25).

3.3.2. Determination and experimental validation of the optimal conditions

Optimization process was carried out to determine the optimum condition to maximize value of K_{La} . According to the software optimization step, to achieve the maximum performance, each of operational

conditions (pH, Q_{air} , Q_{water} , and C_0) was chosen “within the range”, while the response (K_{La}) was defined as “maximum”. The optimum working condition K_{La} and overall liquid mass transfer coefficient K_L are presented in Table 5.

Table 5

A comparison between experimental and predicted K_{La} and K_L under various optimum working conditions.

Solutions Number	Parameters				K_{La} (h^{-1})		K_L (m/min) $\times 10^{-5}$	
	pH (-)	Q_{air} (mL/min)	Q_{water} (mL/min)	C_0 (mg/L)	Predicted	Experimental	Predicted	Experimental
1	12.9	588.53	5.5	378.94	0.733	0.716	3.79	3.70
2	12.7 6	590.7	5.56	384.35	0.730	0.725	3.77	3.74
3	12.9 7	594.87	4.83	381.22	0.731	0.729	3.78	3.76
4	12.9	592.16	5.67	369.69	0.733	0.731	3.79	3.78
5	12.9 5	587.96	5.24	387.38	0.738	0.726	3.81	3.75

As it is shown in Table 5, the highest values of K_{La} , $0.733 h^{-1}$ were predicted according to the model under optimized operational conditions: pH 12.9; Q_{air} 588.53 mL/min; Q_{water} 5.5 mL/min; C_0 378.94 mg/L. An additional experiment was then performed to

confirm the optimum results. These results approve the predictability of the model in the employed experimental conditions. As represented in Table 5, experimental values were reasonably close to the predicted values.

4. Conclusions

By providing a proper condition of mass transfer at interface of gas-liquid phases, microchannel led to the enhancement of the air stripping of ammonia from wastewater. The results of the study showed that all the parameters (pH, Q_{air} , Q_{water} and C_0) have increasing effect on $K_{L,a}$. The effect of increasing pH from 10 to 12.25 obviously increased $K_{L,a}$, around 0.47 h^{-1} . Increasing the air flow rate from 280 to 700 mL/min caused the enhancement of the amount of $K_{L,a}$ from 0.24 to 0.61 h^{-1} . Changing wastewater flow rate in the range of 0.25 to 7.5 mL/min increased the values of $K_{L,a}$ about 160 %. The effect of initial concentration of ammonia on the overall volumetric mass transfer coefficient was evaluated about 20 %. The overall volumetric mass transfer coefficient, $K_{L,a}$ value of 0.730 h^{-1} , was obtained using lower amount of air compared with the other types of the strippers. This efficiency may lead to the development of this application to other stripping systems, which still suffer from low $K_{L,a}$. Because of good mixing in microchannel, it was found that the high amount of $K_{L,a}$ (0.733 h^{-1}) can be obtained by a T-jointed microchannel. In the present study, optimization of the removal of ammonia from wastewater with air stripping in microchannel was investigated. The optimization of stripping process concentrated on the influence of operating variables such as the flow rates of air and wastewater, initial ammonia concentration, and pH using RSM with CCD. The results of the study show that the most effective parameters in the ammonia removal are the air and wastewater flow rate. Initial ammonia concentration and pH were found to be less effective. The optimum results indicated that the optimized operational conditions are: pH 12.9;

$Q_{\text{air}}=588.53 \text{ mL/min}$; $Q_{\text{water}}=5.5 \text{ mL/min}$; $C_0=378.94 \text{ mg/L}$. In this condition, $K_{L,a}$ value of 0.733 h^{-1} was obtained. This study shows the higher capability of the microchannel compared with the stirred tanks and packed towers for ammonia and some volatile chemicals removal of wastewater by desorption process, already developed in the literature.

Nomenclature

a	interfacial area per unit volume of liquid [m^2/m^3].
A	code of pH in Central Composite Design.
B	code of air flow rate in Central Composite Design.
C	code of wastewater flow rate in Central Composite Design.
C_0	initial ammonia concentration [mg/L].
C_{A0}	liquid phase concentration of compound A at the beginning of experiment [g/m^3].
C_{At}	liquid phase concentration of compound A at any time of experiment [g/m^3].
D	code of initial ammonia concentration in Central Composite Design.
H_A	dimensionless Henry's constant.
k	number of studied factors.
K_L	overall liquid mass transfer coefficient [m/min].
	overall volumetric mass transfer coefficient [h^{-1}].
$K_{L,a}$	
Q_{air}	air flow rate [mL/min].
Q_G	gas flow rate [L/min].
Q_{water}	wastewater flow rate [mL/min].
R^2	the coefficient of determination.
t	stripping time [min].
V_L	total volume of liquid [L].
X	variables of quadratic model.
Y	response of quadratic model.

Greek letters

α	axial points for Central Composite
----------	------------------------------------

	Design.
β_0	constant coefficient of quadratic model.
β_j	interaction coefficients of linear terms in quadratic model.
β_{ij}	interaction coefficients of second-order terms in quadratic model.
β_{ij}	dual interaction between investigating parameters.

References

- [1] Değermenci, N., Ata, O. N. and Yildiz, E., "Ammonia removal by air stripping in a semi-batch jet loop reactor", *Ind. Eng. Chem.*, **18** (1), 399 (2012).
- [2] Bonmati, A. and Flotats, X. , "Air stripping of ammonia from pig slurry: Characterisation and feasibility as a pre- or post-treatment to mesophilic anaerobic digestion", *Waste manag.*, **23** (3), 261 (2003).
- [3] Cheung, K. C., Chu, L. M. and Wong, M. H., "Ammonia stripping as a pretreatment for landfill leachate", *Water, Air, Soil Pollut.*, **94** (1-2), 209 (1997).
- [4] Minocha, V. K. and Rao, A. P., "Ammonia removal and recovery from urea fertilizer plant waste", *Environ. Technol.*, **9** (7), 655 (1988).
- [5] Bolado-Rodríguez, S., García-Sinovas, D. and Álvarez-Benedí, J., "Application of pig slurry to soils: Effect of air stripping treatment on nitrogen and TOC leaching", *J. Environ. Manage.*, **91** (12), 2594 (2010).
- [6] Quan, X., et al., "Simultaneous removal of ammonia, P and COD from anaerobically digested piggery wastewater using an integrated process of chemical precipitation and air stripping", *J. Hazard. Mater.*, **178** (1), 326 (2010).
- [7] Djebbar, Y. and Narbaitz, R., "Improved Onda correlations for mass transfer in packed towers", *Water Sci. Technol.*, **38** (6), 295 (1998).
- [8] Basakcildan-Kabakci, S., Ipekoglu, A. N. and Talinli, I., "Recovery of ammonia from human urine by stripping and absorption", *Environ. Eng. Sci.*, **24** (5), 615 (2007).
- [9] Quan, X., et al., "Air stripping of ammonia in a water-sparged aerocyclone reactor", *J. Hazard. Mater.*, **170** (2), 983 (2009).
- [10] Cypes, S. H. and Engstrom, J., "Analysis of a toluene stripping process: A comparison between a microfabricated stripping column and a conventional packed tower", *Chem. Eng. J.*, **101** (1), 49 (2004).
- [11] Vankayala, B. K., et al., "Scale-up of process intensifying falling film microreactors to pilot production scale", *Int. J. Chem. Reactor Eng.*, **5** (1), Article A91, (2007).
- [12] Wenn, D. A., Shaw, J. E. and Mackenzie, B., "A mesh microcontactor for 2-phase reactions", *Lab on a Chip*, **3** (3), 180 (2003).
- [13] Chambers, R. and Spink, R. H., "Microreactors for elemental fluorine", *Chem. Commun.*, **10**, 883 (1999).
- [14] De Bellefon, C., et al., "Asymmetric catalytic hydrogenations at micro-litre scale in a helicoidal single channel falling film micro-reactor", *Catal. Today*, **110** (1), 179 (2005).
- [15] Moschou, P., et al., "Nitrogen stripping of isopropyl-alcohol and toluene in a falling film micro reactor: Gas side mass transfer experiments and modelling at isothermal conditions", *Chem. Eng. Sci.*, **76**, 216 (2012).

- [16] Sun, X., Constantinou, A. and Gavriilidis, A., "Stripping of acetone from isopropanol solution with membrane and mesh gas-liquid contactors", *Chem. Eng. Process.*, **50** (10), 991 (2011).
- [17] Almasvandi, M. H., Rahimi, M. and Tagheie, Y., "Microfluidic cold stripping of H₂S from crude oil in low temperature and natural gas consumption", *J. Natural Gas Sci. Eng.*, **34**, 499 (2016).
- [18] Zhang, X., Stefanick, S. and Villani, F. J., "Application of microreactor technology in process development", *Org. Process Res. Dev.*, **8** (3), 455 (2004).
- [19] Brandt, J. C. and Wirth, T., "Controlling hazardous chemicals in microreactors: Synthesis with iodine azide", *Beilstein J. Org. Chem.*, **5** (1), 30 (2009).
- [20] Sun, J., et al., "Synthesis of biodiesel in capillary microreactors", *Ind. Eng. Chem. Res.*, **47** (5), 1398 (2008).
- [21] Guan, G., et al., "Transesterification of sunflower oil with methanol in a microtube reactor", *Ind. Eng. Chem. Res.*, **48** (3), 1357 (2009).
- [22] Guan, G., et al., "Two-phase flow behavior in microtube reactors during biodiesel production from waste cooking oil", *AIChE J.*, **56** (5), 1383 (2010).
- [23] Basiri, M., Rahimi, M. and Mohammadi, H. B., "Ultrasound-assisted biodiesel production in microreactors", *Iranian J. Chem. Eng.*, **13** (2), 23 (2016).
- [24] Mahjoob, M., Etemad, S. G. and Thibault, J., "Numerical study of non-newtonian flow through rectangular microchannels", *Iranian J. Chem. Eng.*, **6** (4), 45 (2009).
- [25] Niu, H., et al., "Flow pattern, pressure drop, and mass transfer in a gas- liquid concurrent two-phase flow microchannel reactor", *Ind. Eng. Chem. Res.*, **48** (3), 1621 (2008).
- [26] Chen, J. F., et al., "High-throughput microporous tube-in-tube microreactor as novel gas-liquid contactor: Mass transfer study", *AIChE J.*, **57** (1), 239 (2011).
- [27] Su, H., et al., "Mass transfer characteristics of H₂S absorption from gaseous mixture into methyldiethanolamine solution in a T-junction microchannel", *Sep. Purif. Technol.*, **72** (3), 326 (2010).
- [28] Bashir, M. J., et al., "Application of response surface methodology (RSM) for optimization of ammoniacal nitrogen removal from semi-aerobic landfill leachate using ion exchange resin", *Desalination*, **254** (1), 154 (2010).
- [29] Kikutani, Y., et al., "Circulation microchannel for liquid-liquid microextraction", *Microchimica Acta*, **164** (3-4), 241 (2009).
- [30] Hossini, H., et al., "Optimizing ammonia volatilization by air stripping from aquatic solutions using response surface methodology (RSM)", *Desalination and Water Treat.*, (ahead-of-print), 1 (2015).
- [31] Xu, J., et al., "Enhancement of mass transfer performance of liquid-liquid system by droplet flow in microchannels", *Chem. Eng. J.*, **141** (1), 242 (2008).
- [32] N. Kashid, M., Renken, A. and Kiwi-Minsker, L., "Influence of flow regime on mass transfer in different types of microchannels", *Ind. Eng. Chem. Res.*, **50** (11), 6906 (2011).
- [33] Boogar, R. S., Gheshlaghi, R. and Mahdavi, M. A., "The effects of viscosity, surface tension, and flow rate on gasoil-water flow pattern in

- microchannels”, *Korean J. Chem. Eng.*, **30** (1), 45 (2013).
- [34] Rahimi, M., et al., “Optimization of biodiesel production from soybean oil in a microreactor”, *Energy Convers. Manage.*, **79**, 599 (2014).
- [35] Kumar, V., Paraschivoiu, M. and Nigam, K., “Single-phase fluid flow and mixing in microchannels”, *Chem. Eng. Sci.*, **66** (7), 1329 (2011).
- [36] Gaddis, E. and Vogelpohl, A., “The impinging-stream reactor: A high performance loop reactor for mass transfer controlled chemical reactions”, *Chem. Eng. Sci.*, **47** (9), 2877 (1992).
- [37] Petruccioli, M., et al., “Aerobic treatment of winery wastewater using a jet-loop activated sludge reactor”, *Process Biochem.*, **37** (8), 821 (2002).
- [38] Yildiz, E., et al., “High strength wastewater treatment in a jet loop membrane bioreactor: Kinetics and performance evaluation”, *Chem. Eng. Sci.*, **60** (4), 1103 (2005).
- [39] Jain, D., et al., “Liquid circulation characteristics in jet loop reactors”, *Can. J. Chem. Eng.*, **68** (6), 1047 (1990).
- [40] Amirkhani, L., Moghaddas, J. and Jafarizadeh-Malmiri, H., “Optimization of *Candida rugosa* Lipase immobilization parameters on magnetic silica aerogel using adsorption method”, *Iranian J. Chem. Eng.*, **13** (3), (2016).
- [41] Doust, A. M., Rahimi, M. and Feyzi, M., “An optimization study by response surface methodology (RSM) on viscosity reduction of residue fuel oil exposed ultrasonic waves and solvent injection”, *Iranian J. Chem. Eng.*, **13** (1), (2016).
- [42] Shafiee, M., et al., “Preparation of ultra high molecular weight polyethylene using Ziegler-Natta catalyst system: Optimization of parameters by response surface methodology”, *Iranian J. Chem. Eng.*, **11** (1), (2014).
- [43] Wu, Y., Li, Q. and Li, F., “Desulfurization in the gas-continuous impinging stream gas-liquid reactor”, *Chem. Eng. Sci.*, **62** (6), 1814 (2007).
- [44] Sawyer, C. and McCarty, P., *Chemistry for environmental engineers*, New York. Mc Graw-Hill Book Company, (1978).
- [45] Huang, J. C. and Shang, C., *Air stripping*, in *Advanced physicochemical treatment processes*, Springer, p. 47 (2006).
- [46] Design-Expert-Software, www.statease.com, *Trial version*, Last seen at 1 November, (2015).
- [47] Al-Shamrani, A., James, A. and Xiao, H. “Separation of oil from water by dissolved air flotation”, *Colloids Surf., A: Aspects*, **209** (1), 15 (2002).
- [48] Körbahti, B. K. and Tanyolaç, A., “Electrochemical treatment of simulated textile wastewater with industrial components and Levafix Blue CA reactive dye: Optimization through response surface methodology”, *J. Hazard. Mater.*, **151** (2), 422 (2008).
- [49] Ölmez, T., “The optimization of Cr (VI) reduction and removal by electrocoagulation using response surface methodology”, *J. Hazard. Mater.*, **162** (2), 1371 (2009).
- [50] Joglekar, A. M., et al., “Product excellence through experimental design”, *Food Product and Development: From Concept to the Marketplace*, 211 (1987).
- [51] Myers, R. H., Montgomery, D. C. and Anderson-Cook, C. M., *Response surface methodology: Process and product optimization using designed experiments*, Vol. 705, John Wiley & Sons, (2009).